REGULAR ARTICLE

blood advances

Diffuse large B-cell lymphomas in adults with aberrant coexpression of CD10, BCL6, and MUM1 are enriched in *IRF4* rearrangements

Leonie Frauenfeld,[1,*] Natalia Castrejon-de-Anta,[2,*] Joan Enric Ramis-Zaldivar,[3,4] Sebastian Streich,[1] Julia Salmerón-Villalobos,[3,4] Franziska Otto,[1] Annika Katharina Mayer,[1] Julia Steinhilber,[1] Magda Pinyol,[2] Barbara Mankel,[1] Colleen Ramsower,[5,6] Irina Bonzheim,[1] Falko Fend,[1] Lisa M. Rimsza,[5,6] Itziar Salaverria,[3,4] Elias Campo,[2-4,†] Olga Balagué,[2-4,†] and Leticia Quintanilla-Martinez[1,7,†]

[1]Institute of Pathology and Neuropathology, Eberhard Karls University of Tübingen and Comprehensive Cancer Center, University Hospital Tübingen, Tübingen, Germany; [2]Hematopathology Unit, Hospital Clínic de Barcelona, Barcelona, Spain; [3]Institut d'Investigacions Biomèdiques August Pi i Sunyer (IDIBAPS), Barcelona, Spain; [4]Centro de Investigación Biomédica en Red de Cáncer (CIBERONC), Madrid, Spain; [5]Department of Research, and [6]Department of Laboratory Medicine and Pathology, Mayo Clinic, Phoenix, AZ; and [7]Cluster of Excellence iFIT (EXC 2180), University of Tübingen, Tübingen, Germany

Key Points

- DLBCL in adults aberrantly coexpressing CD10, BCL6, and MUM1 is genetically heterogeneous and enriched in *IRF4*-rearranged cases.
- *IRF4*-rearranged DLBCL in adults share genetic features with LBCL-*IRF4* in children but with higher genomic complexity and often ABC GEP.

Diffuse large B-cell lymphoma (DLBCL) with aberrant coexpression of $CD10^+BCL6^+MUM1^+$ (DLBCL-AE), classified as germinal center B cell (GCB) type by the Hans algorithm (HA), was genetically characterized. To capture the complexity of DLBCL-AE, we used an integrated approach that included gene expression profiling (GEP), fluorescence in situ hybridization, targeted gene sequencing, and copy number (CN) arrays. According to GEP, 32/54 (59%) cases were classified as GCB-DLBCL, 16/54 (30%) as activated B-cell (ABC) DLBCL, and 6/54 (11%) as unclassifiable. The discrepancy between HA and GEP was 41%. Three genetic subgroups were identified. Group 1 included 13/50 (26%) cases without translocations and mainly showing and ABC/MCD molecular profile. Group 2 comprised 11/50 (22%) cases with *IRF4* alterations (DLBCL-*IRF4*), frequent mutations in *IRF4* (82%) and NF-κB pathway genes (*MYD88*, *CARD11*, and *CD79B*), and losses of 17p13.2. Five cases each were classified as GCB- or ABC-type. Group 3 included 26/50 (52%) cases with 1 or several translocations in *BCL2/BCL6/MYC*/IGH, and GCB/EZB molecular profile predominated. Two cases in this latter group showed complex *BCL2/BCL6/IRF4* translocations. DLBCL-*IRF4* in adults showed a similar copy number profile and shared recurrent *CARD11* and *CD79B* mutations when compared with LBCL-*IRF4* in the pediatric population. However, adult cases showed higher genetic complexity, higher mutational load with frequent *MYD88* and *KMT2D* mutations, and more ABC GEP. *IRF4* mutations were identified only in *IRF4*-rearranged cases, indicating its potential use in the diagnostic setting. In conclusion, DLBCL-AE is genetically heterogeneous and enriched in cases with *IRF4* alterations. DLBCL-*IRF4* in adults has many similarities to the pediatric counterpart.

Introduction

Diffuse large B-cell lymphoma (DLBCL) is the most common subtype of non-Hodgkin lymphoma, representing ~30% to 40% of all newly diagnosed lymphomas.[1] DLBCL is clinically, morphologically, and biologically a heterogeneous disease reflected in its highly variable clinical course.[2,3] The 2017 World Health Organization (WHO) lymphoma classification recognizes within the group of DLBCL several subtypes characterized by unique clinical, pathological, or genetic features. Nevertheless, most cases of

Submitted 27 August 2021; accepted 16 September 2021; prepublished online on *Blood Advances* First Edition 15 October 2021; final version published online 7 April 2022. DOI 10.1182/bloodadvances.2021006034.

*L.F. and N.C.-d.-A. contributed equally to this study.

†E.C., O.B., and L.Q.-M. supervised this study equally.

The full-text version of this article contains a data supplement.

DLBCL fall into the "not otherwise specified" category. Gene expression profiling (GEP) studies have revealed that DLBCL, not otherwise specified, comprises molecular groups that reflect either the stage in B-cell development from which the disease originates or the activity of different biological programs.[4-8] This cell-of-origin (COO) classification recognizes 2 broad categories: the germinal center B cell (GCB)-like DLBCL, and the activated B cell (ABC)-like DLBCL; however, ~15% remains unclassified.[5,9]

More recently, a genetic classification of DLBCL based on mutational profile, somatic copy-number alterations (CNA), and structural variants was proposed.[3,10,11] The similarities of the molecular subtypes identified in 3 different studies indicate that these subgroups reflect true biological differences. The MCD/C5/MYD88 subtypes are part of the ABC group and are enriched for *MYD88*^{L265P} and *CD79B* mutations with subsequent activation of the NF-κB pathway. The EZB/C3/BCL2 subtypes are assigned to the GCB group and are characterized by *BCL2* translocations and *EZH2* mutations associated with other mutations of chromatin modifiers. In contrast, the BN2/C1/NOTCH2 subtypes, mostly assigned to ABC-DLBCL, are characterized by *BCL6* translocations and *NOTCH2* mutations with a putative origin in marginal zone B cells. The C2 subgroup is defined by *TP53* mutations, a high number of CNAs, and increased ploidy. Based on these molecular studies, a predictor model has been developed that dissects and stratifies further the COO classification into 7 genetic subtypes with apparently clinical relevance: 3 mostly related to ABC-type, 3 to GCB-type, and the novel subgroup genetically related to marginal zone lymphoma.[12]

The increasing defining role of genetic alterations in lymphoma classification is highlighted in the recognition of 2 provisional entities in the 2017 WHO classification, namely, large B-cell lymphoma with *IRF4* rearrangement (LBCL-*IRF4*) and Burkitt-like lymphoma with 11q aberration.[13,14] Burkitt-like lymphoma with 11q aberration is a high-grade B-cell lymphoma without *MYC* translocation and genetic alterations closer to those found in GCB-DLBCL.[15,16] LBCL-*IRF4* predominates in children and young adults, shows frequent involvement of the Waldeyer's ring and gastrointestinal tract, and shows excellent outcome in patients after chemotherapy.[13,17-19] A recent study demonstrated that LBCL-*IRF4* in children and young adults has a distinct molecular profile different from other LBCL characterized by frequent mutations in *IRF4* and NF-κB–related genes (*CARD11*, *CD79B*, and *MYD88*), despite a GCB-transcriptional program, and losses in 17p13 and gains of chromosome 7 and 11q12.3-q25.[20] LBCL-*IRF4* shows mostly a GCB phenotype according to the Hans algorithm (HA),[21] with expression of CD10 (60%) and BCL6 but with strong MUM1/IRF4 expression.[13,19,22] An unanswered question is whether all DLBCLs with aberrant coexpression of CD10, BCL6, and MUM1 (DLBCL-AE) correspond to the GCB subtype and/or carry an *IRF4* translocation. Furthermore, LBCL-*IRF4* has been reported in the adult population[13,23,24]; however, it is not clear whether these cases represent clinically and biologically the same disease with excellent prognosis as in children and young adults.

The aim of this study was to unravel the molecular landscape of 55 cases of DLBCL-AE in an adult population. The analysis revealed that DLBCL-AE is genetically a heterogeneous group enriched in *IRF4*-rearranged (DLBCL-*IRF4*) cases. The clinical and relevant molecular features of DLBCL-*IRF4* in adults were compared with LBCL-*IRF4* in the pediatric population.

Material and methods

Patients and samples

Fifty-five cases of de novo DLBCL aberrantly coexpressing CD10, BCL6, and MUM1/IRF4 (DLBCL-AE) in >50% of tumor cells were included in the study. Initially, 210 cases of DLBCL were investigated and 30 cases of DLBCL-AE (14%) were identified. To expand the study, further cases were collected from different institutions. In total, there were 25 cases from the University of Tübingen, Germany, 20 cases from Hospital Clinic of Barcelona, Spain, and 10 cases from the Mayo Clinic, Phoenix, Arizona. As control, 9 cases of DLBCL were included: 5 with GCB phenotype and 4 with non–GCB phenotype according to HA. The cases were classified following the criteria of the 2017 WHO classification.[25] The immunohistochemical staining was performed as part of the diagnostic workup. The study was approved by the local Ethics Review Committee and the IRB review panels of the contributing institutions (UKT 199/2020BO2). It was conducted in accordance with the Declaration of Helsinki.

Fluorescence in situ hybridization

Fluorescence in situ hybridization (FISH) analyses for the detection of *BCL2*, *BCL6*, *MYC*, *IRF4*, IGH, IGK, and IGL translocations were performed using LSI Dual color break-apart probes (Metasystems, Altlußheim, Germany; Agilent Technologies, Santa Clara, CA; Vysis-Abbott Molecular, Wiesbaden, Germany). In some cases, homemade FISH probes were used.[13] For the triple-color FISH IGH-*BCL2*-*IRF4*, the XL t(14;18) IGH/*BCL2* dual fusion probe (Metasystems) was cohybridized with BAC clones spanning the *IRF4* loci RP3-416J7, RP5-1077H22, and RP5-856G1 labeled in Spectrum Aqua.

Targeted next generation sequencing (NGS) and mutational analysis

The mutational status of 66 B-cell lymphoma–related genes (supplemental Table 1) was investigated using a SureSelectXT Target Enrichment System Capture NGS strategy library (Agilent Technologies) before sequencing in a MiSeq equipment (Illumina, San Diego, CA) (supplemental Methods). As verification, 25 cases were additionally investigated with a 10-gene Ion AmpliSeq Custom panel (supplemental Table 2) (Ion Torrent S5; Thermo Fisher Scientific). The Custom Panel was designed using the Ion AmpliSeq Designer from Thermo Fisher Scientific (version 3.4). For description of library preparation, sequencing, and raw data analyses see supplemental Methods. The previously published mutational profile of 17 pediatric and young adult cases of LBCL-*IRF4* was used for comparison.[20] Occurrence of mutations in genes within predefined pathogenic pathways was calculated per each molecular group.[26]

DNA CN alterations analysis

CN alterations were examined in LBCL-*IRF4* and/or *IRF-4* mutated using Oncoscan (Thermo Fisher Scientific), according to standard protocols (supplemental Methods). Gains and losses and CN neutral loss of heterozygosity (CNN-LOH) regions were evaluated using Nexus Biodiscovery version 9.0 software (Biodiscovery, Hawthorne, CA). Additional previously published CN data were used for comparison.[20]

Gene expression analysis (NanoString and HTG)

COO classification was performed using the Lymph2Cx assay (NanoString, Seattle, WA) and/or HTG EdgeSeq System (HTG Molecular Diagnostics Inc., Tucson, AZ) (supplemental Methods). *IRF4* mRNA levels were established based on the number of counts of *IRF4*_NM_002460.1 on the Lymph2Cx assay.

Statistical methods

Differences in the distribution of individual parameters among patient subsets were analyzed by Fisher's exact test for categorized variables and the Student *t*-test for continuous variables. The *P* values for multiple comparisons were adjusted using the Benjamini-Hochberg correction (false discovery rate). A cutoff of $P = .05$ was considered significant. Statistical analyses were performed using R software version 3.5.0.

Results

Clinical and morphological findings

Clinical information is summarized in Table 1 and supplemental Table 3. A total of 55 patients were included in the study, of whom 22 were male and 33 were female patients, representing a M:F ratio of 1:1.5 with a median age of 70 years (range 37-92 years). Twenty-three patients (42%) showed nodal presentation whereas 32 patients (58%) had extranodal presentation, with 10 cases (18%) involving the tonsils/Waldeyer's ring, 6 cases involving the gastrointestinal tract (11%), 3 cases (5%) involving the testis, and 2 cases each (4%) involving bone marrow and breast and others (16%). Of the patients with available clinical information, 19/45 had low-stage disease at presentation (42%) whereas 26/45 patients had high-stage disease (58%). Thirty patients (30/48; 62%) were alive at last follow-up without evidence of disease, with a median follow-up of 36 months (range 7-97 months). Ten patients died; 9 died of disease with a median of 7 months (range 1-21 months), and 1 patient died after 6 months of an unrelated cause. Eight patients were lost to follow-up during or after therapy (range 0-19 months).

Table 1. Clinical data of 55 patients with DLBCL with aberrant coexpression of CD10, BCL6, and MUM1

Parameter	No. of cases
Age	Mean 70 y (range 37-92 y)
Male gender	22 (40%)
Female gender	33 (60%)
Stage I/II	19/45 (42%)
Stage III/IV	26/45 (58%)
Localization	
Nodal presentation	23 cases (42%)
Extranodal presentation	32 cases (58%)
Tonsil/Waldeyer's ring	10 cases (18%)
Gastrointestinal tract	6 cases (11%)
Testis	3 cases (5%)
Breast	2 cases (4%)
Other	11 cases (20%)
Alive, no evidence of disease	30/48 patients (62%)
Median follow-up (range)	36 mo (7-97 mo)
Died of disease	9/48 patients (19%)
Median (range)	7 mo (1-21 mo)
Cell of origin	
GCB	32/54 (59%)
ABC	16/54 (30%)
UC	6/54 (11%)

UC, unclassifiable.

Morphologically, 6 cases revealed a blastoid cytology (Figure 1A), whereas 49 cases showed a characteristic centroblastic cytology (Figure 1B). All cases showed expression of CD10, BCL6, and MUM1/IRF4 in more than 50% of tumor cells (Figure 1C-E).

FISH results

The results of FISH analysis for *BCL2*, *BCL6*, *MYC*, *IRF4*, and IG genes are summarized in supplemental Table 4. Of the 55 cases, 15 cases (27%) showed no rearrangements whereas 40 cases (73%) showed 1 or more rearrangements (Figure 1F-H). The most frequently rearranged genes were *BCL2* and *BCL6* (12 cases each) followed by *IRF4* and *MYC* (11 cases each). Two cases were double-hit (*MYC/BCL6*), 2 cases were triple-hit (*MYC/BCL2/BCL6*), and 4 cases showed rearrangements of both *BCL2* and *BCL6*. IGH was detected as the translocation partner in 23 cases whereas in 2 cases IGL was demonstrated. In 6 cases, an IG break was detected (4 IGH, 1 IGL, and 1 IGK) without identifiable partner. Of the 11 cases with *IRF4* rearrangement, 2 cases (cases 25 and 26) also had a *BCL2* and/or a *BCL6* translocation. Because of the complex rearrangements, these 2 cases were further analyzed.

Triple-color FISH IGH-*BCL2*-*IRF4* on case 25 showed that all cells had rearrangements of *BCL2* and *IRF4* and colocalized with IGH locus in the same derivative chromosome (Figure 2A). This derivative chromosome containing these 3 loci was duplicated. These results suggest that in case 25, a t(6;14;18) translocation occurred as 1 hit.

FISH constellation in case 26 showed typical patterns of break for IGH and *IRF4* loci, whereas *BCL2* break-apart probes revealed 3 clones with different *BCL2* rearrangements: the first clone with a typical *BCL2* break, the second clone with a gain of normal chromosome 18 to the break, and the third clone with loss of 3' signal (red signal) in derivative chromosome 18 (Figure 2B). Using triple-color FISH *IGH-BCL2-IRF4*, *IRF4* locus did not colocalize with either the IGH locus or the t(14;18) derivative chromosomes, indicating that *IRF4* rearrangement was an independent, clonal alteration observed in more than 80% of the cells.

Gene expression patterns

GEP was performed in 54 cases: 48 cases with the Lymph2Cx, and 24 cases with HTG EdgeSeq DLBCL COO assay (supplemental Table 4). In 18 cases, both techniques were performed. According to GEP, 32/54 (59%) cases were classified as GCB, 16/54 (30%) were classified as ABC, and 6/54 (11%) were unclassifiable. The correlation between the 2 different assays was very good (13/

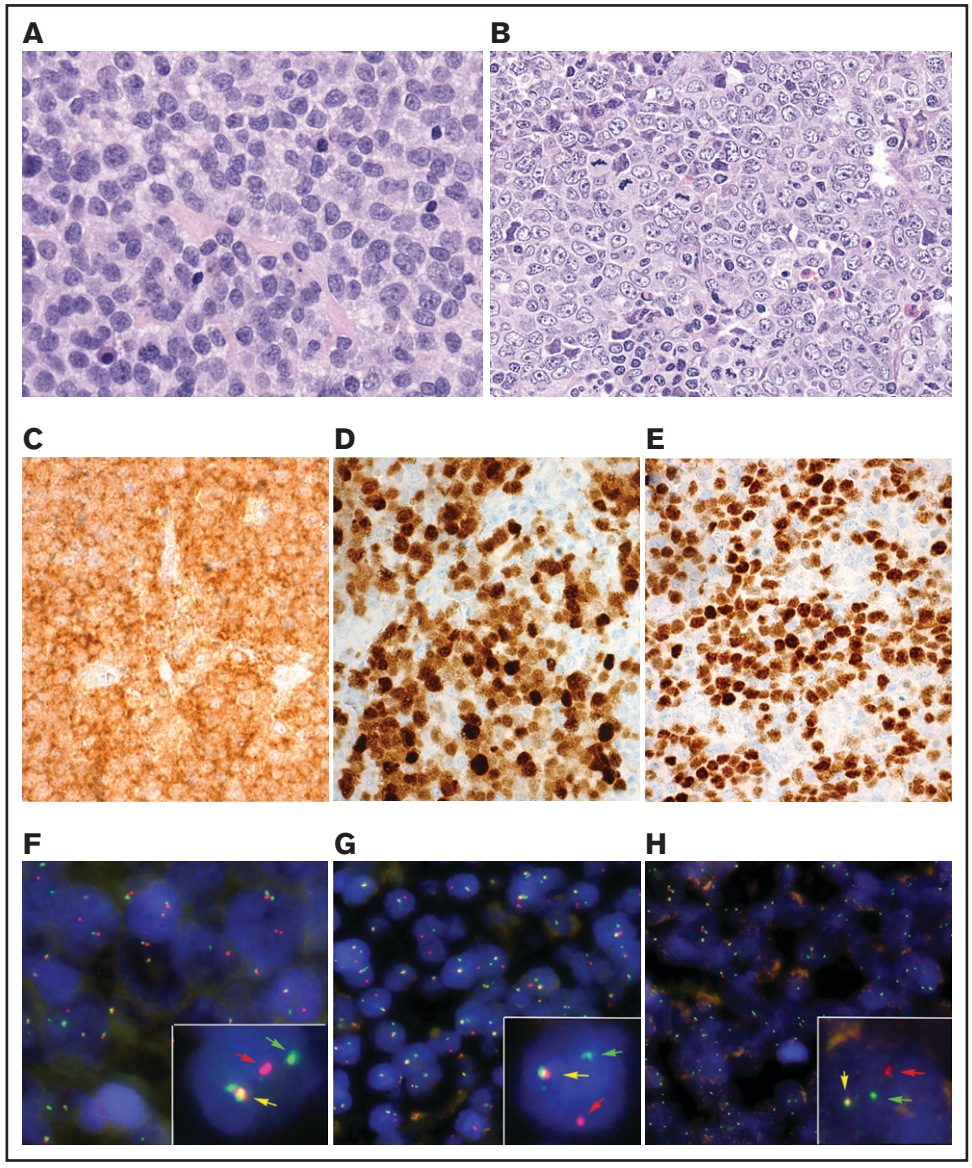

Figure 1. Morphological, immunophenotypic, and genetic features of triple-positive DLBCLs. (A) B-cell lymphoma with blastic morphology characterized by medium- to large-sized cells with irregular nuclei, fine chromatin, inconspicuous nucleolus, and scant cytoplasm (case 10), (original magnification ×400; hematoxylin and eosin stain). (B-G) Case 5 shows a characteristic centroblastic morphology (original magnification ×400; hematoxylin and eosin stain). The tumor cells are $CD10^+$ (C), $MUM1/IRF4^+$ (D), and $BCL6^+$ (E) (original magnification ×400; immunostaining). FISH demonstrates an *IRF4* (F) and IGL (G) break with 1 colocalized signal (yellow arrow) and 1 split signal (green and red arrows) consistent with gene rearrangement. (H) In case 2, an IGK break was demonstrated. FISH shows a signal constellation of 1 colocalized signal (yellow arrow) and 1 split signal (green and red arrows) consistent with gene rearrangement.

18; 72%). No discordant cases were classified as GCB or ABC; however, in 5 cases assigned as unclassifiable by the Lymph2Cx, HTG EdgeSeq classified 3 as ABC and 2 as GCB. The discrepancy between the HA and GEP in the DLBCL-AE was 41%. In contrast, in the control cases there was a 100% agreement between HA and GEP (supplemental Figure 1).

Identification of recurrent mutations by NGS

All cases were analyzed by next generation sequencing (NGS). Fifty cases were informative, of which 46 were analyzed with the 66-gene SureSelectXT panel (mean coverage 873; range 26-2693) and 24 were analyzed with the 10-gene Ampliseq panel (mean coverage 1650; range 100-65 280). Twenty cases were analyzed with both panels and 4 cases only with the Ampliseq panel (supplemental Table 5). In the 50 evaluable cases, 531 mutations were identified in 47 (94%) whereas in 3 cases (6%) no mutations were identified (mean 10.62 mutations/case). A total of 392 variants (74%) were predicted as potential driver mutations with a mean of 7.84 mutations per case. The most recurrently mutated genes were *KMT2D* and *PIM1* (19/50; 38%) followed by *MYD88* (17/50; 34%); *CREBBP* (14/50; 28%); *HIST1H1E* (11/50; 22%); *BTG2*, *TP53* (10/50; 20%); *IRF4*, *SOCS1* (8/50; 16%); *BCL2*, *CARD11*, *TET2* (7/50;14%); *BTG1*, *ARID1A*, *TBLXR1* (6/50; 12%); *MYC*, *EP300*, *TNFRSF14*,

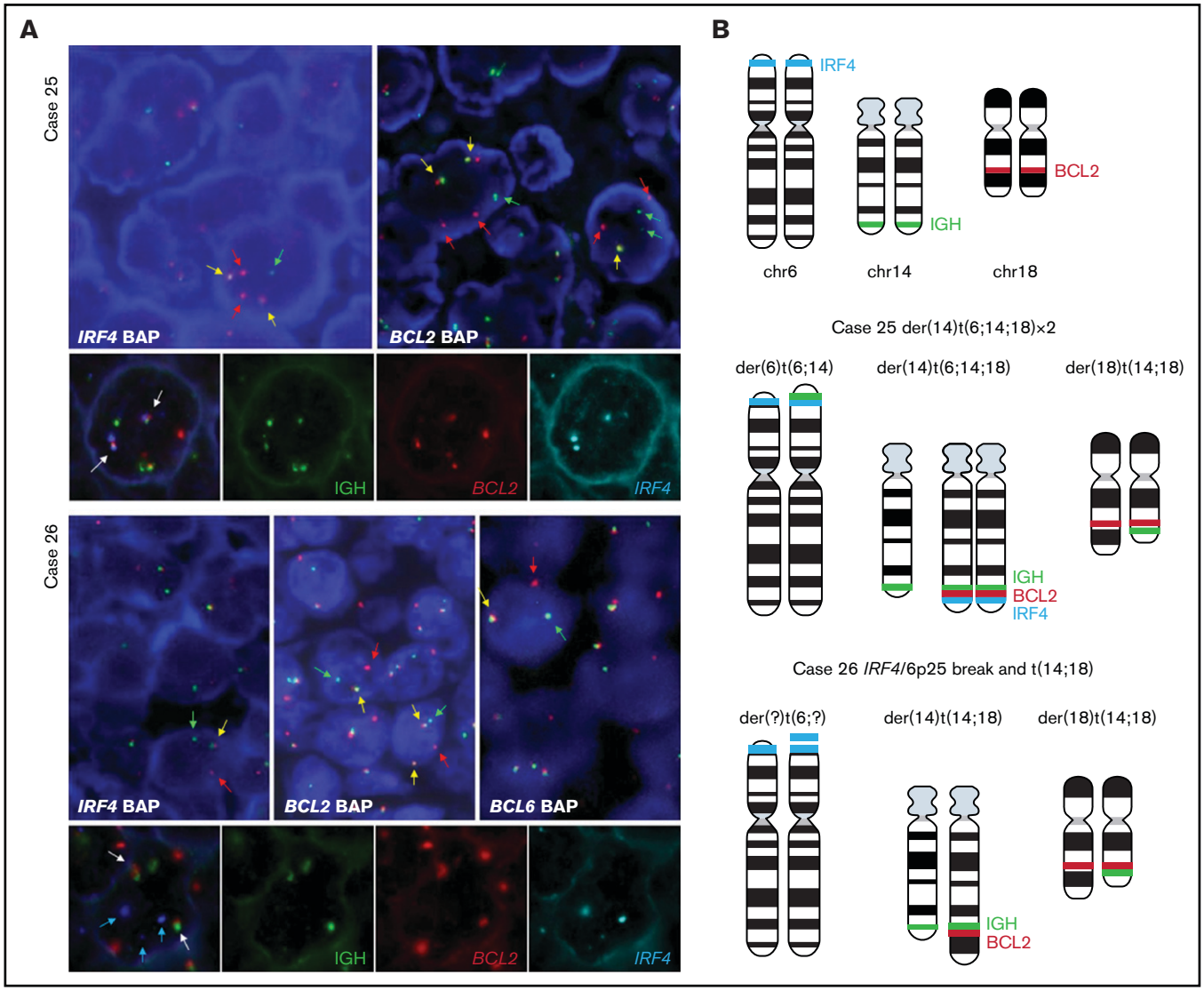

Figure 2. FISH analysis demonstrates complex rearrangement with *IRF4* and *BCL2/BCL6* genes. (A) FISH analyses using *IRF4*, *BCL2*, and *BCL6* break-apart probes and triple-color FISH for IGH, *BCL2*, and *IRF4* loci in the 2 cases with *IRF4* rearrangement together with *BCL2* in case 25 and *BCL2/BCL6* rearrangement in case 26. These hybridizations were performed using t(14;18) dual-color fusion (Metasystems) and BAC clones spanning *IRF4* locus (BAC clones 5' RP3-416J7 and 3' RP5-1077H22 and RP5-856G1) labeled in spectrum aqua. Red signals correspond to *BCL2*, green signals correspond to IGH, and aqua/blue signals represent *IRF4*. Case 25. FISH demonstrates *IRF4* and *BCL2* breaks (upper panel) with 1 or 2 colocalized signals (yellow arrows) and 1 or 2 split signals (green and red arrows) consistent with *BCL2* and *IRF4* gene rearrangement. The triple rearrangement (IGH-*IRF4*-*BCL2*) (lower panel) is demonstrated by colocalization of the 3 colors (white arrows). Case 26. FISH analysis for *IRF4*, *BCL2*, and *BCL6* with break-apart probes demonstrates 1 colocalized signal (yellow arrow) and 1 split signal (green and red arrows), indicating a triple rearrangement. FISH analyses of concomitant IGH, *BCL2* and *IRF4* rearrangements (lower panel) show 2 colocalized signals (white arrow) of the derivative chromosomes 14 and 18 resulting in t(14;18) translocation. *IRF4* locus (blue arrows) did not colocalize with either the IGH locus or the t(14;18) translocation, indicating that this is an independent rearrangement with unknown partner. (B) Schematic representation of *IRF4* (aqua blue), IGH (green), and *BCL2* (red) breaks/rearrangements in cases 25 and 26.

TMEM30A, *PRKCB*, *BCL10*, *CD79B*, *SGK1*, *ETS1* (5/50%; 10%); and others (Figure 3).

MYD88 gene mutations were mostly identified in the hotspot p.L265P; however, in 4/17 cases, variant mutations were observed (p.S219C, p.D148V, p.S243N, p.S149N), all of which were predicted as driver mutations. Multiple *IRF4* mutations were identified in 4 of 8 cases, including synonymous variants. These mutations were exclusively found in the highly conserved *N*-terminal DNA-binding domain. In 2 additional cases (cases 26 and 44), only 1 *IRF4* mutation was identified but predicted as passenger. All *IRF4* mutations were exclusively identified in *IRF4*-rearranged cases. Multiple mutations in >3 cases were identified in *IRF4* and *PIM1*. The pattern of these mutations is concordant with aberrant somatic hypermutation (aSHM) (supplemental Table 6). In the 20 cases analyzed with both panels, 67 mutations were verified (89%), whereas 8 mutations (5 *PIM1*, 1 *BCL2*, and 2 *IRF4*) were only identified with the SureSelectXT panel.

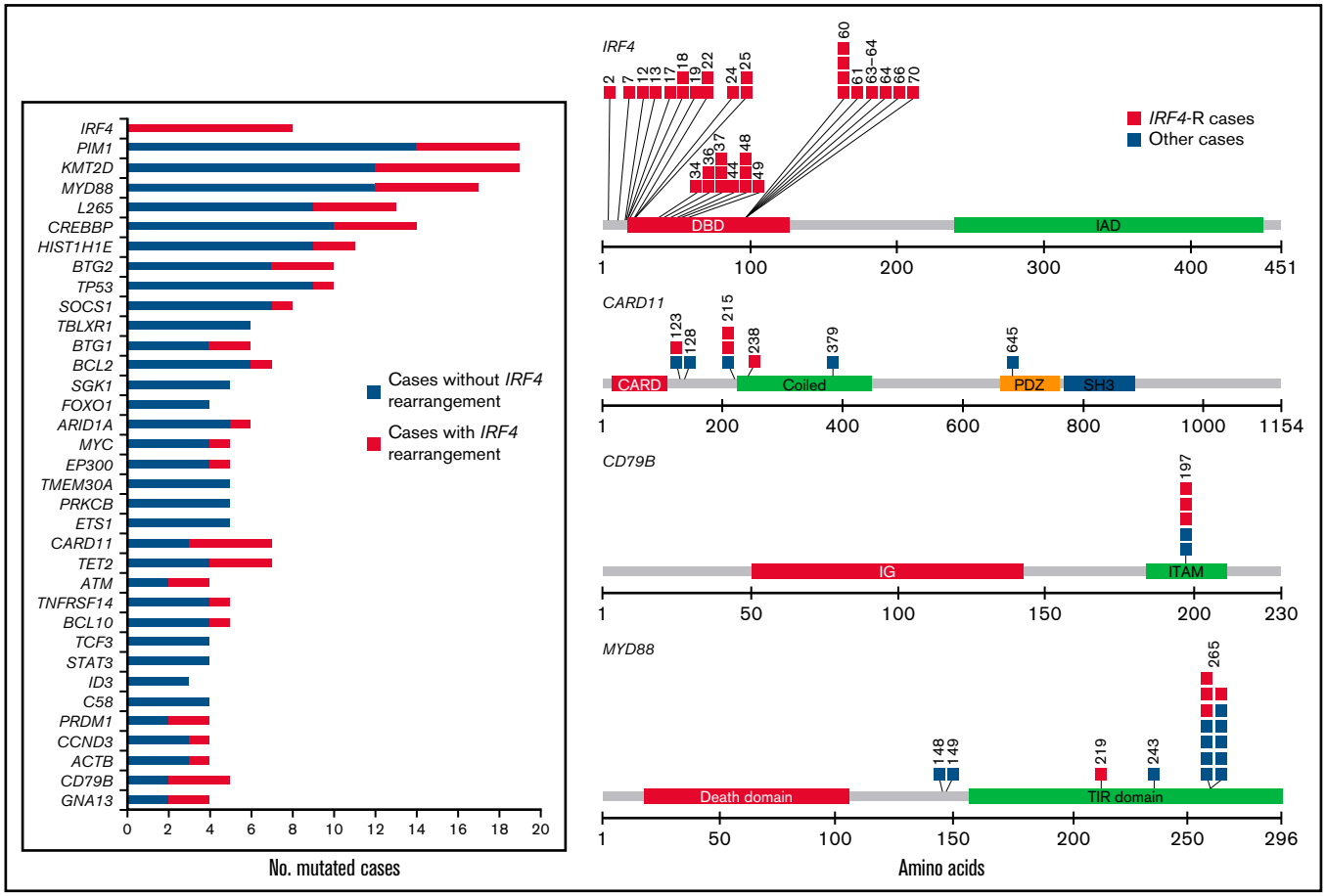

Figure 3. Mutational landscape of 50 cases of DLBCL-AE. Bar graph shows mutated genes in 4 or more cases. The results are given in number of mutated cases per gene. The colored bars indicate the presence (orange) or absence (blue) of *IRF4* rearrangement. A diagram of the relative positions of driver mutations is shown for *IRF4*, *CARD11*, *CD79B*, and *MYD88*. Multiple passenger mutations for *IRF4* also are depicted. The x-axis indicates amino acid positions. The approximate location of somatic mutations identified in each gene is indicated. *IRF4* mutations are mainly in the DNA binding domain. All *CD79B* mutations are located in a hotspot Y197 in the immunoreceptor tyrosine-based activation motif (ITAM). Domains of the protein are represented according to the Uniprot database (www.uniprot.org).

Molecular subgroup prediction

Molecular subgroup prediction of 46 DLBCL-AE cases was performed using the LymphGen tool.[12] Only information on 42/114 genes used by the algorithm was available. This algorithm predicted 57% of the cases to belong to 1 of the molecular subgroups. Most cases were predicted as belonging to either the MCD group (24%) or the EZB group (17%), with few cases belonging to the BN2 (7%), ST2 (4%), MCD/ST2 (2%), and BN2/EZB/MCD (2%) groups (Figure 4A).

Correlation of clinical features, FISH, GEP, and mutational analysis

Based on primary events detected by FISH, 3 groups were recognized (Figure 5). Five cases without mutational analysis were excluded. Group 1 included 13/50 cases (26%) without translocations. There were 7 male and 6 female patients with a median age of 70 years (range 38-84 years). Eight cases (54%) were GCB-type whereas 7 cases were ABC-type (46%). In total, 66 driver mutations were identified with a mean of 5.5 mutations/case. The MCD mutational profile predominated in this group (6/12; 50%). Interestingly, 3 cases assigned to the GCB group by GEP (case 7 with HTG, case 15 with HTG and NanoString, and case 57 with NanoString) carried *MYD88* and *CD79B* mutations and were predicted to belong to the MCD molecular subgroup. Summing the molecular subgroup and GEP, 9 cases (60%) showed ABC/MCD profile. Group 2 included 11/50 (22%) cases of DLBCL with *IRF4* rearrangements (DLBCL-*IRF4*). In 2 cases, no *IRF4* break was demonstrated; however, these 2 cases had a light chain IG break and *IRF4* mutations indicating a cryptic *IRF4* rearrangement. The group consisted of 3 male and 8 female patients with a median age of 67 years (range 37-85 years). From the 10 cases analyzed for GEP, 5 cases were subclassified as GCB and 5 as ABC. In total, 96 driver mutations (mean 10.7 mutations/case) were identified. Four cases were predicted as MCD mutational profile and 1 was assigned to the ST2 group. This group was characterized by 1 or multiple *IRF4* mutations (82%) and frequent *MYD88* (45%), *CARD11* (36%), and *CD79B* (27%) mutations. Finally, group 3 included 26/50 cases (52%) with 1 or several translocations in *BCL2*/*BCL6*/*MYC*/IGH. The 2 cases with complex *BCL2* and/or *BCL6* translocations together with *IRF4* were included in this group. There were 9 male and 17 female patients with a median

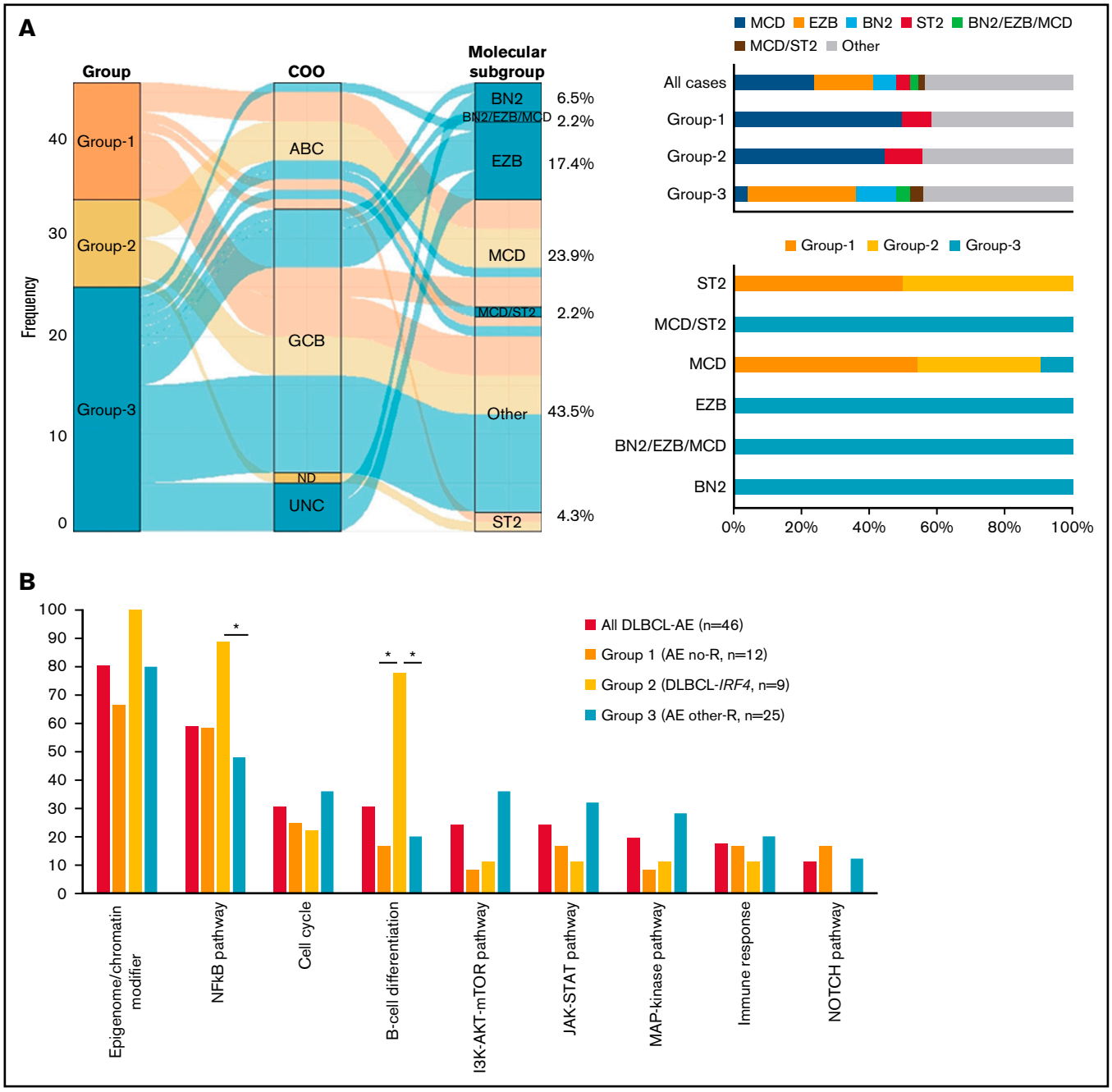

Figure 4. Molecular subgroup prediction and recurrent mutated pathways in DLBCL-AE. (A) Alluvial plot shows the frequency and relationship between groups, COO classification according to LYMPH2Cx, and/or HTG and molecular subgroup prediction according to *LymphGen* tool[12] of 46 cases of DLBCL-AE. The bars indicate the molecular predicted subgroup in all cases and in each genetic group identified; 57% of all cases were assigned to a specific molecular subgroup. (B) Recurrent mutated pathways[22] in 46 cases of DLBCL-AE. Genes included in each pathway are indicated in supplemental Table 1. Bar graph shows the total number of mutated cases for each pathway. Asterisk represents significant mutated pathways. AE, aberrant expressor $CD10^+BCL6^+MUM1^+$; R, rearrangement.

age of 68 years (range 44-87 years). In this group, the GCB-type (16/26; 62%) and the EZB-type (8/25; 32%) mutational profile predominated. In total, 219 driver mutations were identified, with a mean of 8.8 mutations/case.

The presence of recurrent mutated pathways was evaluated in the 3 groups (Figure 4B). This analysis showed significantly more mutations in NF-κB pathway and B-cell differentiation genes in group 2 (DLBCL-*IRF4*) when compared with the other 2 groups ($P < .05$). Group 2 also carried more driver mutations per case when compared with group 1 (10.7 vs 5.5 driver/case; Wilcoxon, $P = .01$) and group 3 (10.7 vs 8.84 driver/case; Wilcoxon, $P = .33$) with significantly more *IRF4*, *CARD11*, and *CD79B* mutations ($P < .05$).

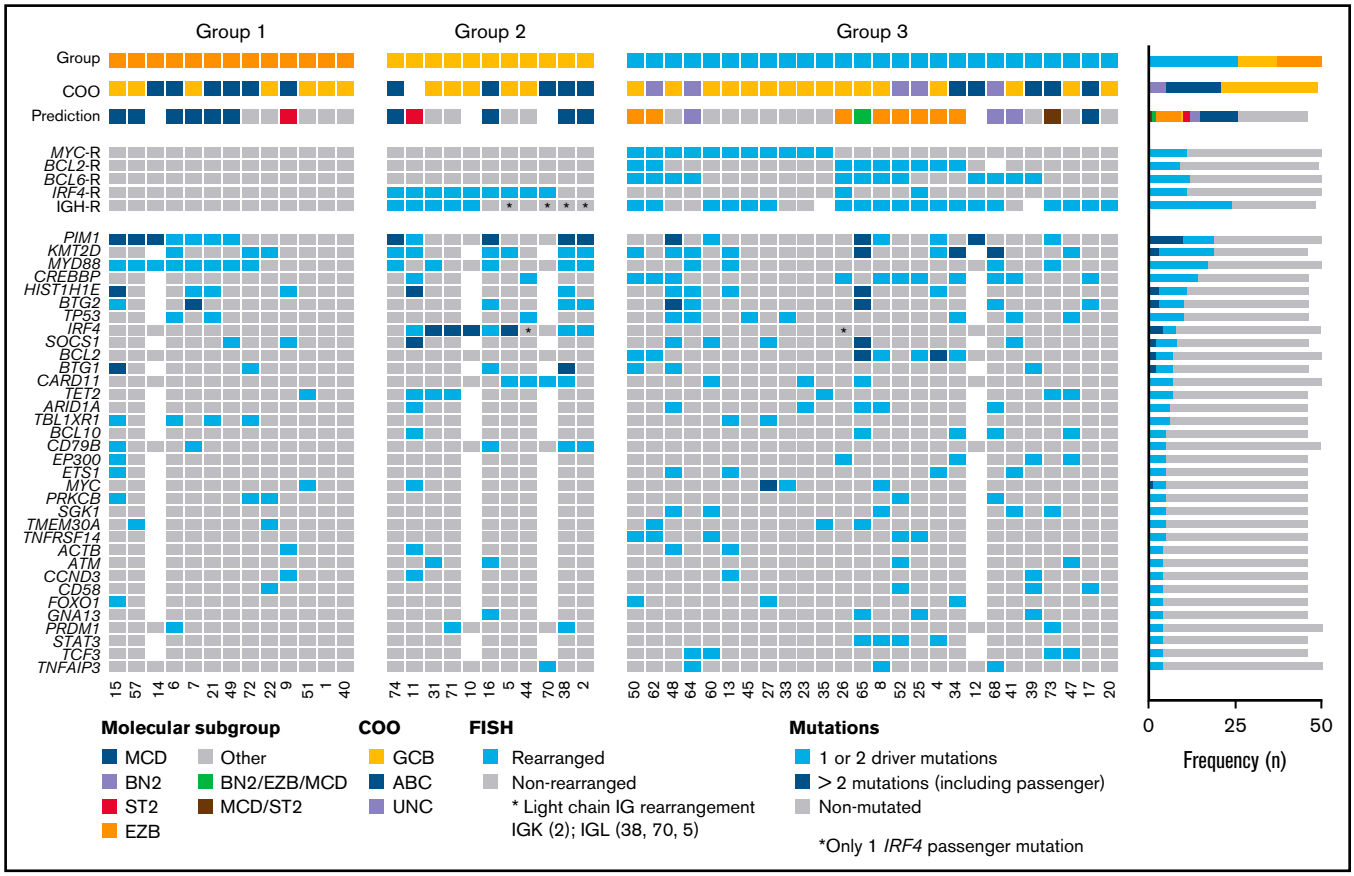

Figure 5. Overview of 50 cases of DLBCL with aberrant coexpression of CD10, BCL6, and MUM1 clustered in 3 groups. Oncoprint includes FISH results, molecular subgroup prediction according to *LymphGen* tool, COO classification according to Lymph2Cx, and/or HTG and frequently mutated genes (>3 cases). Each column of the plot represents 1 TP case and each line is a specific analysis. On the right side of the figure, the frequency of the particular result of the analysis is shown.

The clinical parameters including sex, age, and overall survival did not differ in the 3 groups (supplemental Table 7; supplemental Figure 2). These results were also observed when a correlation analysis was performed, including the clinical features and molecular characteristics of the 3 groups (mutations >4 cases) (supplemental Figure 3).

CN results of DLBCL-*IRF4* cases in adults

CN analysis of 7 DLBCL-*IRF4* revealed a total of 118 genetic alterations (mean 17 alterations per case; range, 0-63 alterations) (Figure 6A; supplemental Table 8). Specifically, 62 CN losses, 43 CN gains, 8 homozygous deletions, and 5 high-copy gains were detected. The most recurrent alterations were 17p13.2 losses detected in 71% of cases (5/7 cases), including *TP53* locus in all 5 cases. Additional frequent alterations observed were CN gain of 18q22.3-q23 and CN loss of 6q23.3-q24.1. Twenty-one regions of CNN-LOH were detected in 6 cases, with 11p11.2-p11.12 being the most recurrently affected region. Case 74 presented a complex genetic profile, with 63 regions of CNA and a chromothripsis-like pattern in chromosome 13. Interestingly, it harbored homozygous deletion of chromosome 6q23.3, encompassing *TNFAIP3* gene.

Cases with *IRF4* rearrangement together with *BCL2* (case 25) and *BCL2/BCL6* (case 26) rearrangements were also analyzed. They displayed a complex CN profile (22 and 24 regions of CNA) but were not higher than the cases with only *IRF4* rearrangement. Interestingly, case 25 presented a CN gain in chromosome 18q21.33, with *BCL2* locus in the breakpoint where the gain starts, supporting the presence of the rearrangement. Case 26 harbored CN loss of 17p13 but *TP53* was not included in that alteration; instead, it was encompassed in a region of CN gain.

Comparison between pediatric and adult *IRF4*-rearranged cases

The comparison of CN profile between DLBCL-*IRF4* in adults and previously published LBCL-*IRF4* data in pediatric population (20 cases) (Figure 6A) showed no differences in terms of recurrent CN-altered regions; however, adult cases showed higher genetic complexity (16.85 alt/case in adults vs 6.25 alt/case in pediatric cases; $P = .33$), and more ABC COO ($P = .05$). Although there is a considerable difference in the genetic complexity based on CN alterations, it was not statistically significant, probably because of the small size of the compared groups.

Similarly, mutational comparison between DLBCL-*IRF4* in adults ($n = 9$) and previously published profiles in children ($n = 17$) (Figure 6B) showed higher mutational load in adult cases (10.7 vs 4.7 mutations/case; Wilcoxon test, $P = .004$) with higher frequency of *KMT2D*, *MYD88*, and *BTG2* mutations (Fisher's exact test; $P < .05$).

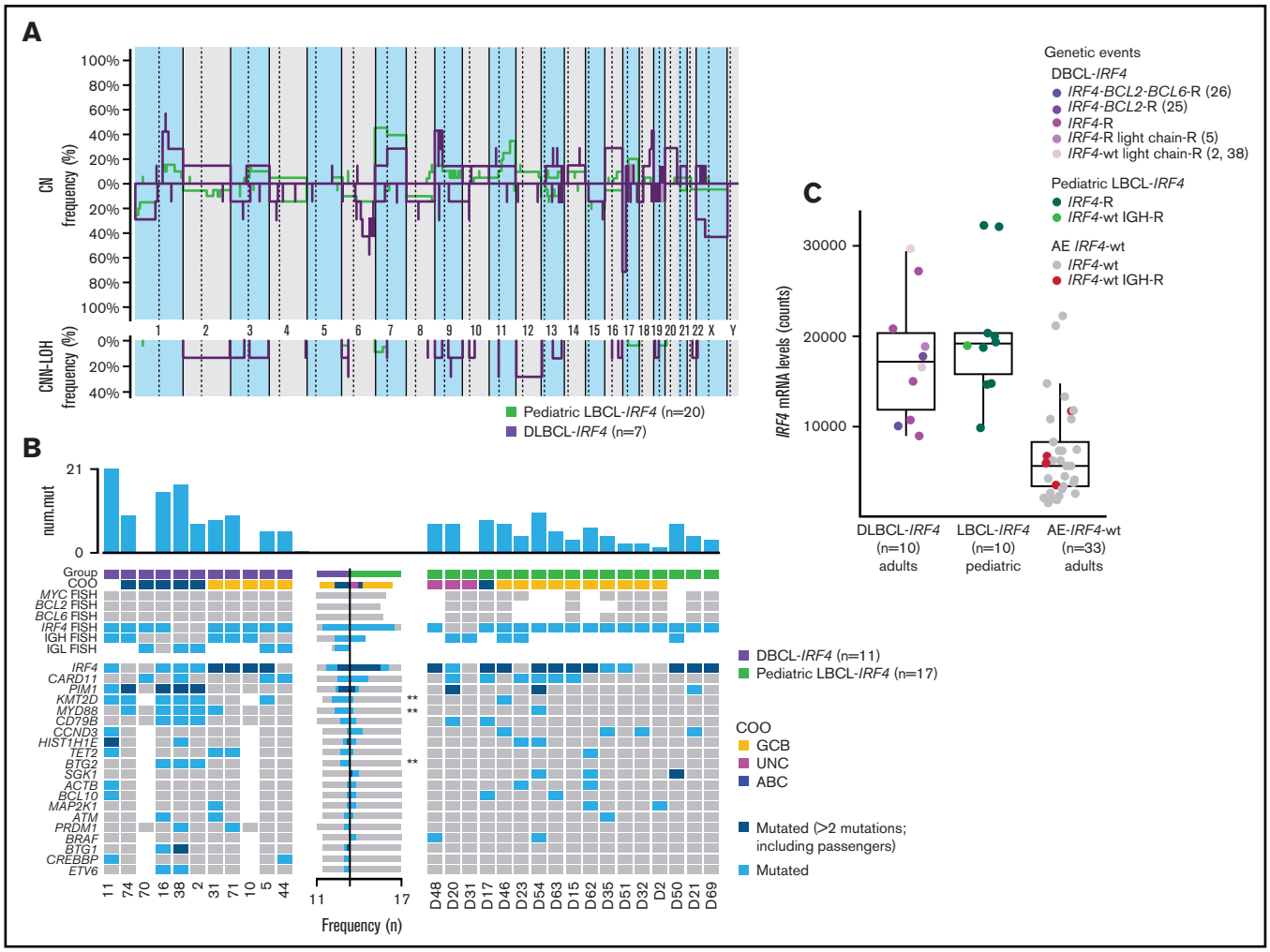

Figure 6. Comparison of CN profile and genetic features of adult and pediatric LBCL-*IRF4* cases. (A) Comparative plot of CN and CNN-LOH between 7 LBCL-*IRF4* cases in adults and 20 LBCL-*IRF4* cases in the pediatric population. No significantly different regions were identified. (B) GEP and mutational comparison between LBCL-*IRF4* in adults (n = 11) and previously published profiles in children (n = 17) showed ABC COO more often ($P = .05$) in adults, with higher mutational load (10.6 vs 4.7 mutations/case; Wilcoxon test, $P = .004$) and higher frequency of *KMT2D*, *MYD88*, and *BTG2* ($P < .05$, marked with asterisk). (C) *IRF4* mRNA expression levels obtained from the IRF4_NM_002460.1 probe on the Lymph2Cx assay. *IRF4* mRNA levels in LBCL-*IRF4* in children and adults was similar but higher when compared with DLBCL-AE without *IRF4* rearrangement (17 570 vs 6948; Wilcoxon test, $P \leq .01$). AE, aberrant expressor CD10$^+$BCL6$^+$MUM1$^+$; R, rearrangement; wt, wild-type.

IRF4 mRNA expression levels were obtained from the IRF4_NM_002460.1 probe on Lymph2Cx assay and compared between DLBCL-*IRF4* in adults (n = 10), DLBCL-AE without *IRF4* rearrangement (n = 33), and pediatric LBCL-*IRF4* (n = 10) (Figure 6C). *IRF4*-rearranged cases in adults and children had similar *IRF4* mRNA levels (number of counts; 17 570 vs 20 155; Wilcoxon test, $P < .44$), which was higher than those observed in DLBCL-AE without *IRF4* rearrangement (number of counts; 17 570 vs 6948; Wilcoxon test, $P \leq .01$).

Discussion

In this study, we comprehensively characterized the molecular features of 55 DLBCL cases with aberrant coexpression of CD10, BCL6, and IRF4/MUM1 that, according to the HA, belong to the GCB-type of DLBCL. We now demonstrate that DLBCL-AE is genetically heterogeneous and 41% (22/54) of the cases show either an ABC-type GEP or are unclassifiable, contributing to the discordant results between GEP and HA.[21,27] These findings clearly indicate that DLBCL-AE should not be classified with the HA. An important aspect of the study was to demonstrate that DLBCL-AE is enriched in cases carrying *IRF4* alterations (13/55; 24%).

Recent studies have shown that to capture the complexity of DLBCL, an integrative multilayer analysis is needed that includes GEP, mutational profile, chromosomal translocations, and CNAs.[3,10-12] Accordingly, this multiplatform approach in DLBCL-AE identified 3 genetic subgroups. Group 1 included cases without chromosomal translocations and, despite expressing CD10, often showed GEP and/or mutational profile of ABC/MCD subgroup. Although MCD usually lacks GCB signature expression,[12] we identified 3 cases with GCB-type GEP and MCD mutational landscape, indicating a clear discrepancy between genotype and phenotype of the tumor cells. Cases similar to these were not captured in the recently described genetic classification[12]

highlighting the challenges that present the extreme genetic and phenotypic heterogeneity of DLBCL for the development of precision therapy.

Group 2 was composed of cases with only *IRF4* chromosomal translocation, including 2 cases with putative cryptic *IRF4* translocations.[20,22] In 5 cases, IGH was the partner of the translocation, whereas in 4 cases a break in the IG light chain was identified. A hallmark of LBCL-*IRF4* in pediatric cases[20] not observed in other cases of DLBCL[28] is the association of GCB GEP and the presence of 1 or multiple *IRF4* mutations, identified in this study in 82% of the cases. Because *IRF4* mutations show the pattern of aSHM and predominant AID mutational signature,[20,29] its presence is indicative of an *IRF4* translocation and of potential use in the diagnostic setting. An important question is whether cases in adults represent the same disease as in children and young adults (≤25 years).[19,20] The genetic comparison demonstrated that although pediatric and adults cases share the same recurrent altered CN regions and frequent mutations in *IRF4*- and NF-kB–related genes (*MYD88*, *CARD11*, and *CD79B*), as a group, adult cases showed higher genetic complexity, had a higher mutational load (10.7 vs 4.7 mutations/case; Wilcoxon test, $P = .004$) with more *KMT2D*, *MYD88*, *CD79B*, and *BTG2* mutations ($P < .05$), and more often had an ABC-type GEP ($P = .05$).

Interestingly, by dissecting the *IRF4* altered cases into GCB- vs ABC-type, important differences were observed. The 5 cases with GCB GEP showed lower genomic complexity and multiple *IRF4* mutations, confirming that AID-driven aSHM is a GCB hallmark. The molecular prediction did not assign these cases into any of the 7 well-defined molecular subgroups,[12] indicating that these cases have molecular features that distinguish them from other DLBCL. Furthermore, 3 cases (cases 5, 10, and 44) were in patients younger than age 40. Two cases presented in the tonsil and 1 in a submandibular lymph node. All 3 had excellent response to conventional chemotherapy and achieved complete remission. Nevertheless, similar cases can also occur in older patients (cases 31 and 71). In contrast, most elderly patients with *IRF4* alterations showed an ABC GEP (5 cases) and carried 1 or no *IRF4* mutations but frequent *KMT2D* (4/5), *MYD88* (4/5), and *BTG2* (3/5) mutations, which are acquired only sporadically as byproducts of aSHM.[30] Recently, it has been shown that ABC-type lymphomas most probably derive from memory B cells that infrequently reenter the GC,[31] explaining why these cases have no or only 1 *IRF4* mutation. However, *KMT2D* mutations are not characteristic of ABC/MCD lymphomas; furthermore, *KMT2D* and *MYD88* mutations are genetic events that increase with age and are rarely observed in the pediatric population.[10] Importantly, in previous studies on DLBCL in adults,[3,10-12] *IRF4*-rearranged cases have not been recognized or evaluated as a group, most probably precluding the correct identification of these cases with available algorithms. Although the number of cases of DLBCL-AE with *IRF4* alterations in the study is relatively low, these findings suggest that patients under 40 years of age and/or with GCB GEP have the same clinical and genetic disease as patients with LBCL-*IRF4* in the pediatric population. This finding supports the contention that molecular characteristics in "pediatric" DLBCL are associated with age and represent a continuum that appears to end close to 40 years of age rather than 18 years of age.[32] In contrast, cases in elderly patients with DLBCL-*IRF4* and *IRF4* mutations, although belonging to the same group, show additional genetic alterations associated with age and are assigned to ABC GEP. Further analysis is warranted to confirm the molecular features of DLBCL-*IRF4* in adults, which might influence treatment strategies in the future. Another important issue is that not all LBCL-*IRF4* cases aberrantly coexpressed CD10, BCL6, and MUM1. Approximately 40% to 50% of the cases are CD10$^-$, making the identification of these cases difficult.[13,19,20,22,33]

Group 3 was composed of DLBCL carrying 1 or several translocations in *BCL2*/*BCL6*/*MYC*/IGH and assigned mainly to the GCB/EZB group. The 3 cases predicted to be in the BN2 molecular subgroup carried BCL6 translocations. The 2 cases with complex chromosomal translocations affecting *IRF4* and *BCL2*/*BCL6* genes were included in this group because in addition to GCB GEP, they showed genetic alterations closer to those found in GCB-DLBCL and were predicted to be in the EZB molecular group.

In conclusion, we have demonstrated that cases of DLBCL-AE are genetically heterogeneous. An important novel finding was that 24% of these cases carried an *IRF4* alteration. Furthermore, DLBCL-*IRF4* in adults has some similarities but also important differences from its pediatric counterpart. Our data suggest that within the group of *IRF4*-rearranged cases in adults, there are genetic features similar to LBCL-*IRF4* disease in children and young adults, with some differences inherent to the aging process. Cases with complex *IRF4* translocations with *BCL2* or *BCL2*/*BCL6* genes have the molecular characteristics of GCB/BCL2/EZB-type DLBCL and should not be included in the group of DLBCL-*IRF4* in adults. Cases of DLBCL-AE show different genetic features that may impact therapeutic strategies, emphasizing the value of molecular subtyping in DLBCL.

Acknowledgments

The authors thank Claudia Hermann, Esther Kohler, Noelia García, Elena Gonzalvo, and Ingrid López for the excellent technical assistance.

This work was supported in part by the Deutsche Forschungsgemeinschaft (DFG) under Germany's Excellence Strategy (iFIT) EXC2180-390900677 (L.Q.-M.); the Ministerio de Ciencia e Innovación (MCI) grant No. RTI2018-094274-B-I00 (E.C.); EDER: European Regional Development Fund "Una manera de hacer Europa" and Generalitat de Catalunya Suport Grups de Recerca AGAUR grant Nos. 2017-SGR-1142 (E.C.) and 2017-SGR-1107 (I.S.); Acció instrumental d'incorporació de científics i tecnòlegs PERIS 2016 (SLT002/16/00336) and Asociación Española Contra el Cáncer (AECC CICPFI6025SALA) (I.S.). E.C. is an academia researcher of the Institució Catalana de Recerca I Estudis Avançats of the Generalitat de Catalunya (ICREA). I.S. is a Miguel Servet researcher (CPII18/00015) from Instituto de Salud Carlos III.

Authorship

Contribution: L.Q.-M., E.C., and O.B. conceived and designed the study; S.S., B.M., I.S., J.S.-V., and L.F. performed the FISH analysis; J.E.R.-Z., F.O., A.K.M., J.S., and I.B. performed NGS mutational analysis; M.P., F.O., S.S., and L.F. performed the GEP analysis; J.S.-V.

and I.S. performed the CNA analysis; L.M.R. and C.R. contributed material; L.Q.-M., E.C., O.B., F.F., L.F., and N.C.-d.-A. reviewed the cases; I.B., F.O., and I.S. supervised the experimental work; L.Q.-M., O.B., and I.S. wrote the manuscript; and L.F., N.C.-d.-A., E.C., and F.F. helped write the manuscript.

Conflict-of-interest disclosure: E.C. and L.M.R. are co-inventors of the Lymph2Cx gene expression profiling assay used in this study. The remaining authors declare no competing financial interests.

ORCID profiles: N.C.-d.-A., 0000-0002-0647-3058; S.S., 0000-0002-7334-1565; I.S., 0000-0002-2427-9822; E.C., 0000-0001-9850-9793; L.Q-M., 0000-0001-7156-5365.

Correspondence: Leticia Quintanilla-Martinez, Institute of Pathology, University Hospital Tübingen, Liebermeisterstr 8, 72076 Tübingen, Germany; e-mail: leticia.quintanilla-fend@med.uni-tuebingen.de; and Olga Balagué, Pathology Department, Hematopathology Unit, Hospital Clinic de Barcelona, Calle de Villarroel 170, 08036 Barcelona, Spain; e-mail: OBALAGUE@clinic.cat.

References

1. Smith A, Crouch S, Lax S, et al. Lymphoma incidence, survival and prevalence 2004-2014: sub-type analyses from the UK's Haematological Malignancy Research Network. *Br J Cancer.* 2015;112(9):1575-1584.
2. Sehn LH, Gascoyne RD. Diffuse large B-cell lymphoma: optimizing outcome in the context of clinical and biologic heterogeneity. *Blood.* 2015; 125(1):22-32.
3. Lacy SE, Barrans SL, Beer PA, et al. Targeted sequencing in DLBCL, molecular subtypes, and outcomes: a Haematological Malignancy Research Network report. *Blood.* 2020;135(20):1759-1771.
4. Alizadeh AA, Eisen MB, Davis RE, et al. Distinct types of diffuse large B-cell lymphoma identified by gene expression profiling. *Nature.* 2000; 403(6769):503-511.
5. Wright G, Tan B, Rosenwald A, Hurt EH, Wiestner A, Staudt LM. A gene expression-based method to diagnose clinically distinct subgroups of diffuse large B cell lymphoma. *Proc Natl Acad Sci USA.* 2003;100(17):9991-9996.
6. Rosenwald A, Wright G, Chan WC, et al; Lymphoma/Leukemia Molecular Profiling Project. The use of molecular profiling to predict survival after chemotherapy for diffuse large-B-cell lymphoma. *N Engl J Med.* 2002;346(25):1937-1947.
7. Pasqualucci L. The genetic basis of diffuse large B-cell lymphoma. *Curr Opin Hematol.* 2013;20(4):336-344.
8. Ennishi D, Hsi ED, Steidl C, Scott DW. Toward a new molecular taxonomy of diffuse large B-cell lymphoma. *Cancer Discov.* 2020;10(9):1267-1281.
9. Scott DW, Wright GW, Williams PM, et al. Determining cell-of-origin subtypes of diffuse large B-cell lymphoma using gene expression in formalin-fixed paraffin-embedded tissue. *Blood.* 2014;123(8):1214-1217.
10. Chapuy B, Stewart C, Dunford AJ, et al. Molecular subtypes of diffuse large B cell lymphoma are associated with distinct pathogenic mechanisms and outcomes [published correction appears in *Nat Med.*]. *Nat Med.* 2018;24(5):679-690.
11. Schmitz R, Wright GW, Huang DW, et al. Genetics and pathogenesis of diffuse large B-cell lymphoma. *N Engl J Med.* 2018;378(15):1396-1407.
12. Wright GW, Huang DW, Phelan JD, et al. A probabilistic classification tool for genetic subtypes of diffuse large B cell lymphoma with therapeutic implications. *Cancer Cell.* 2020;37(4):551-568.e14.
13. Salaverria I, Philipp C, Oschlies I, et al; Berlin-Frankfurt-Münster-NHL trial group. Translocations activating IRF4 identify a subtype of germinal center-derived B-cell lymphoma affecting predominantly children and young adults. *Blood.* 2011;118(1):139-147.
14. Salaverria I, Martin-Guerrero I, Wagener R, et al; Berlin-Frankfurt-Münster Non-Hodgkin Lymphoma Group. A recurrent 11q aberration pattern characterizes a subset of MYC-negative high-grade B-cell lymphomas resembling Burkitt lymphoma. *Blood.* 2014;123(8):1187-1198.
15. Gonzalez-Farre B, Ramis-Zaldivar JE, Salmeron-Villalobos J, et al. Burkitt-like lymphoma with 11q aberration: a germinal center-derived lymphoma genetically unrelated to Burkitt lymphoma. *Haematologica.* 2019;104(9):1822-1829.
16. Wagener R, Seufert J, Raimondi F, et al. The mutational landscape of Burkitt-like lymphoma with 11q aberration is distinct from that of Burkitt lymphoma. *Blood.* 2019;133(9):962-966.
17. Woessmann W, Quintanilla-Martinez L. Rare mature B-cell lymphomas in children and adolescents. *Hematol Oncol.* 2019;37(suppl 1):53-61.
18. Quintanilla-Martinez L, Sander B, Chan JK, et al. Indolent lymphomas in the pediatric population: follicular lymphoma, IRF4/MUM1+ lymphoma, nodal marginal zone lymphoma and chronic lymphocytic leukemia. *Virchows Arch.* 2016;468(2):141-157.
19. Au-Yeung RKH, Arias Padilla L, Zimmermann M, et al. Experience with provisional WHO-entities large B-cell lymphoma with IRF4-rearrangement and Burkitt-like lymphoma with 11q aberration in paediatric patients of the NHL-BFM group. *Br J Haematol.* 2020;190(5):753-763.
20. Ramis-Zaldivar JE, Gonzalez-Farré B, Balagué O, et al. Distinct molecular profile of IRF4-rearranged large B-cell lymphoma. *Blood.* 2020;135(4):274-286.
21. Hans CP, Weisenburger DD, Greiner TC, et al. Confirmation of the molecular classification of diffuse large B-cell lymphoma by immunohistochemistry using a tissue microarray. *Blood.* 2004;103(1):275-282.
22. Liu Q, Salaverria I, Pittaluga S, et al. Follicular lymphomas in children and young adults: a comparison of the pediatric variant with usual follicular lymphoma. *Am J Surg Pathol.* 2013;37(3):333-343.
23. de Leval L, Bonnet C, Copie-Bergman C, et al. Diffuse large B-cell lymphoma of Waldeyer's ring has distinct clinicopathologic features: a GELA study. *Ann Oncol.* 2012;23(12):3143-3151.
24. Zhou L, Gu B, Shen X, et al. B cell lymphoma with IRF4 rearrangement: a clinicopathological study of 13 cases. *Pathol Int.* 2021;71(3):183-190.

25. Swerdlow SH, Campo E, Harris NL, et al. WHO Classification of Tumours of Haematopoietic and Lymhoid Tissues. Lyon, France: IARC; 2017.
26. Karube K, Enjuanes A, Dlouhy I, et al. Integrating genomic alterations in diffuse large B-cell lymphoma identifies new relevant pathways and potential therapeutic targets. *Leukemia.* 2018;32(3):675-684.
27. Choi WW, Weisenburger DD, Greiner TC, et al. A new immunostain algorithm classifies diffuse large B-cell lymphoma into molecular subtypes with high accuracy. *Clin Cancer Res.* 2009;15(17):5494-5502.
28. Pasqualucci L, Trifonov V, Fabbri G, et al. Analysis of the coding genome of diffuse large B-cell lymphoma. *Nat Genet.* 2011;43(9):830-837.
29. Liu M, Duke JL, Richter DJ, et al. Two levels of protection for the B cell genome during somatic hypermutation. *Nature.* 2008;451(7180):841-845.
30. Venturutti L, Melnick AM. The dangers of déjà vu: memory B cells as the cells of origin of ABC-DLBCLs. *Blood.* 2020;136(20):2263-2274.
31. Mesin L, Schiepers A, Ersching J, et al. Restricted clonality and limited germinal center reentry characterize memory B cell reactivation by boosting. *Cell.* 2020;180(1):92-106.e11.
32. Klapper W, Kreuz M, Kohler CW, et al; Molecular Mechanisms in Malignant Lymphomas Network Project of the Deutsche Krebshilfe. Patient age at diagnosis is associated with the molecular characteristics of diffuse large B-cell lymphoma. *Blood.* 2012;119(8):1882-1887.
33. Chisholm KM, Mohlman J, Liew M, et al. IRF4 translocation status in pediatric follicular and diffuse large B-cell lymphoma patients enrolled in Children's Oncology Group trials. *Pediatr Blood Cancer.* 2019;66(8):e27770.